



Amphiphilic pyrenecarboxylic acids: incorporation into vesicle membrane and ability as sensitizer for electron transport reactions

Ryo Sasaki, Yuki Nako, Shigeru Murata *

Department of Basic Science, Graduate School of Arts and Sciences, The University of Tokyo, Meguro-ku, Tokyo 153-8902, Japan

ARTICLE INFO

Article history:

Received 21 March 2009

Received in revised form 13 July 2009

Accepted 13 July 2009

Available online 16 July 2009

Keywords:

Pyrene derivatives

Amphiphilic molecules

Vesicles

Electron transfer

ABSTRACT

The novel pyrenecarboxylic acids **1–3** having a single or double hydrophobic alkyl chain were synthesized, and their photophysical properties were investigated in solutions and vesicle membranes. In analogy with parent 1-pyrenecarboxylic acid, the absorption and fluorescence spectra of **1–3** were changed with the H^+ concentration. The amphiphilic pyrenecarboxylic acids **1–3** had good solubility in the vesicle membranes, and acted as an excellent sensitizer for the electron transport from an electron donor in the inner waterpool of the vesicle to an electron acceptor in the outer aqueous phase across vesicle membranes.

© 2009 Elsevier Ltd. All rights reserved.

1. Introduction

Pyrene is an aromatic hydrocarbon having unique photophysical characteristics, which include a relatively long lifetime of its singlet excited state and a high quantum yield of fluorescence ($\tau_s=650$ ns and $\phi_f=0.65$ in nonpolar solvents).¹ It is known that the vibronic fine structure of its fluorescence is very sensitive to the polarity of the surrounding medium.² Moreover, pyrene readily forms fluorescent excimers that can be utilized to study its mobility and aggregation behaviors.³ Based on these characteristics, pyrene and its derivatives have been employed widely as probes in the investigation of various multimolecular systems such as polymers,⁴ self-assembled monolayers,⁵ and vesicles.⁶

In addition, pyrene and its derivatives have often been used as sensitizers to initiate electron transfer reactions.⁷ Recently, we reported the pyrene-sensitized electron transport across phosphatidylcholine (PC) vesicle bilayers, in which an endoergic electron transfer from ascorbate (Asc^-) in the inner waterpool of the vesicle to methylviologen (MV^{2+}) in the outer aqueous solution was driven by the irradiation of pyrene derivative embedded in the vesicle bilayers.^{8,9} It was found that a hydrophilic functional group, such as $-CO_2H$, $-NH_2$, and $-OH$, was required for pyrene derivatives to act as sensitizers for the electron transport across vesicle bilayers. Moreover, the sensitizer ability decreased as the length of the methylene chain connecting the hydrophilic group with the

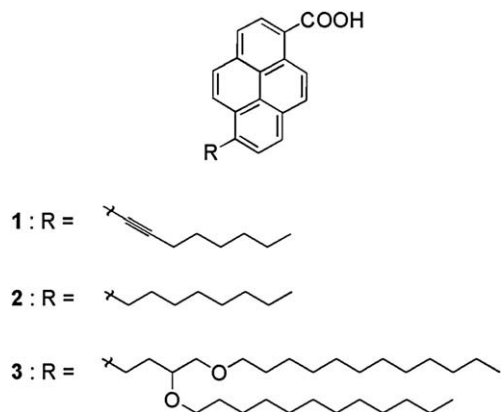
pyrene nucleus was increased: when $PyCH_2CO_2H$, $Py(CH_2)_2CO_2H$, and $Py(CH_2)_3CO_2H$ ($Py=1$ -pyrenyl) were employed as a sensitizer, the relative quantum yields for MV^{2+} formation decreased significantly in that order. These observations are interpreted in terms of the position of the pyrene moiety of the sensitizer relative to the bilayer–water interface. The pyrene moiety connected to a hydrophilic functional group by a short methylene chain is anchored at the bilayer–water interface, facilitating electron transfer processes that occur at the interface. Thus, it is concluded that the use of pyrenes functionalized by a hydrophilic group as a sensitizer is essential to achieve high efficiency of the electron transport across vesicle bilayers.

On the basis of the discussion described above, 1-pyrenecarboxylic acid $PyCO_2H$ in which a carboxyl group is attached directly to the pyrene nucleus would be a promising sensitizer for the electron transport across vesicle bilayers. Although the photophysical properties of $PyCO_2H$ have been the subject of interest over the years,^{10–13} especially in large discrepancies in the dissociation constant between its ground and excited states, no studies of electron transfer reactions sensitized by $PyCO_2H$ were reported. Contrary to our expectation, however, we found that $PyCO_2H$ could not be employed as a sensitizer for the electron transport across vesicle bilayers since it was not incorporated in PC vesicle membranes owing to its high hydrophilicity.⁸ Thus, we decided to design and synthesize pyrenecarboxylic acids having good solubility in the vesicle membranes.

In order to obtain pyrenecarboxylic acids, which can be incorporated in the vesicle membranes, a molecular design to increase the hydrophobicity of $PyCO_2H$, such as an introduction of

* Corresponding author. Tel.: +81 3 5454 6596; fax: +81 3 5454 6998.
E-mail address: cmura@mail.ecc.u-tokyo.ac.jp (S. Murata).

a long alkyl chain into its pyrene nucleus, is required. Although Kano and his co-workers demonstrated the formation of well-ordered monolayer of 8-dodecyl-1-pyrenecarboxylic acid with the aid of glucolipid,¹⁴ few examples of pyrenecarboxylic acids having a hydrophobic group have been reported so far. This paper deals with newly designed three amphiphilic pyrenecarboxylic acids **1–3** and reports their syntheses, photophysical properties in solutions and vesicle membranes, and ability as a sensitizer for the electron transport across vesicle bilayers.



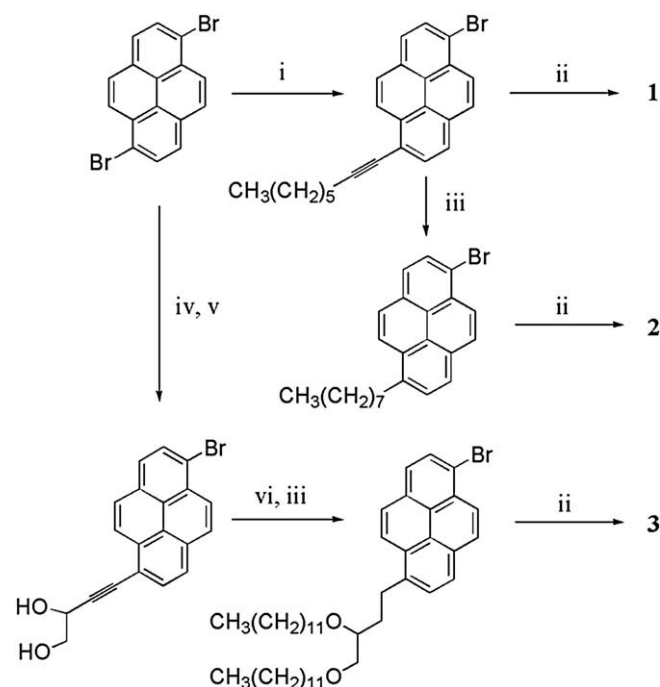
2. Results and discussions

2.1. Design and syntheses of amphiphilic pyrenecarboxylic acids

Recently, we reported the preparation of unsymmetrically substituted bifunctional pyrenes having a carboxyl group linked with an ethylene group and a hydrophobic long alkyl chain using 1,6-dibromopyrene¹⁵ as a starting material.⁹ This dihalide is a reasonable precursor of amphiphilic pyrenecarboxylic acids because the bromine atoms on its pyrene nucleus can be converted into a carboxyl group and an alkyl group through carboxylation and Sonogashira coupling reaction, respectively. Thus, we first designed the pyrenecarboxylic acid **1** having an alkynyl group of standard chain length and its saturated version **2**. Many amphiphilic molecules having a double alkyl chain were synthesized as analogues of natural PC molecules and their aggregation behaviors were investigated in water.¹⁶ Thus, the double-chain amphiphilic pyrenecarboxylic acid **3** was also designed, which would be expected to have a strong affinity for vesicles composed of PC molecules. These amphiphilic pyrenecarboxylic acids **1–3** could be synthesized according to the route summarized in Scheme 1.

2.2. Spectroscopic properties of amphiphilic pyrenecarboxylic acids in solutions

Before the photoinduced electron transport experiments using the amphiphilic pyrenecarboxylic acids **1–3** as sensitizers were carried out, we examined their photophysical properties in solutions first. The spectroscopic properties of parent PyCO₂H that serve to interpret absorption and fluorescence spectra of **1–3** have been extensively investigated,^{10–13} which are summarized as follows. It is well-known that the spectra of PyCO₂H in an acidic medium is considerably different from those in a basic medium. This observation is interpreted in terms of the dissociation of PyCO₂H in aqueous solutions, p*K* of which is reported to be 3.1 or 4.0.^{17,18} The basic form PyCO₂[−] gives a well-structured fluorescence spectrum having the 0,0 transition at 381 nm that resembles that of pyrene in shape, indicating a weak interaction of the carboxylate group with



Scheme 1. Route for the preparation of amphiphilic pyrenecarboxylic acids **1–3**. Reagents and conditions: (i) 1-octyne, PdCl₂(PPh₃)₂, CuI, morpholine; (ii) *n*-BuLi, THF and then CO₂(s); (iii) H₂, PtO₂, EtOAc; (iv) 4-ethynyl-2,2-dimethyl-1,3-dioxolane, PdCl₂(PPh₃)₂, CuI, morpholine; (v) 4 M HCl, THF; (vi) NaH, DMF, and then 1-bromododecane.

the π electrons of the pyrene ring. On the other hand, the fluorescence of the acidic form PyCO₂H is broad and featureless with a maximum at 415 nm. A bathochromic shift in the fluorescence spectrum of the acidic form indicates a higher p*K* of PyCO₂H in the excited state compared with that in the ground state, which can be predicted numerically by Eq. 1 derived from the Förster cycle.¹⁹

$$\Delta pK = pK^* - pK = 0.625 \cdot \Delta\bar{\nu} / T \quad (1)$$

where p*K*^{*} and p*K* represent the dissociation constants of PyCO₂H in the excited and ground state, respectively, $\Delta\bar{\nu}$ is a difference in the 0,0 transition energy in cm^{−1} between the basic and acidic forms, and *T* stands for the temperature in the experimental condition. Using the maximal position of the fluorescence spectrum in an acidic medium, Vender Donckt and his co-workers estimated p*K*^{*} of PyCO₂H to be 8.1.¹⁷ However, this value is controversial because the 0,0 transition energy of the acidic form cannot be determined from its broad and less structured fluorescence spectrum. In fact, it was reported that the acidic form gave a well-structured fluorescence spectrum in a glassy glycerol/water solvent below 150 K, in which the 0,0 transition appeared at 384 nm.¹³ In any event, it should be noted that the fluorescence spectrum of the acidic form is very sensitive to solvent and temperature, in which a broad and featureless peak is observed when the excited state molecule can be relaxed by reorganization of polar solvent molecules. Milosavljevic and Thomas proposed the participation of the protonated form PyCO₂H₂⁺ in the emission spectrum recorded in acidic aqueous solutions.¹⁰ Furthermore, Milosavljevic and Thomas determined a rate constant for the reaction of H⁺ with excited state PyCO₂[−] to be 1.0 × 10¹¹ M^{−1} s^{−1}.¹⁰ It seems that this value is not inconsistent with the observation reported by Zelent and his co-workers that PyCO₂[−] is not converted to PyCO₂H during the excited state lifetime at pH 5.0, indicating that H⁺ at 10^{−5} M concentration does not act as a proton donor for excited state PyCO₂[−].¹² However, they also reported that the addition of sodium acetate to the aqueous solution of PyCO₂[−] at pH 5.0 resulted in an increase in the fluorescence of the acidic form,

which is interpreted in terms of the protonation of excited state PyCO_2^- with acetic acid generated in the solution.

The amphiphilic pyrenecarboxylic acids **1–3** were fairly soluble in organic solvents such as CHCl_3 and methanol. The absorption and fluorescence spectral data obtained in CHCl_3 are summarized in Table 1. The spectra of **2** and **3** were practically identical, while a small bathochromic shift was observed both in the absorption and fluorescence spectra of **1**, which is due to the extension of the π conjugated system by the substitution of the alkynyl group on the pyrene ring. The absorption spectra of **1–3** were broad and less structured, and the peak assigned to the $^1A_g \rightarrow ^1L_b$ transition was observed at 398 nm for **1** and 389 nm for **2** and **3**. These features of the absorption spectra are in agreement with those of the acidic form of parent PyCO_2H , suggesting the amphiphilic pyrenecarboxylic acids are in the acidic form in CHCl_3 solutions. In the fluorescence spectra of **1–3**, a shoulder derived from vibrational structure was observed at 430 nm for **1** and 425 nm for **2** and **3**. In spite of the presence of a long alkyl chain that would induce a nonradiative deactivation of the excited state, the amphiphilic pyrenecarboxylic acids **1–3** exhibited relatively high fluorescence quantum yields of 0.81–0.91, which are slightly greater than 0.75 reported for parent PyCO_2H in deoxygenated CH_2Cl_2 .¹¹

Table 1
Absorption and fluorescence spectral data of amphiphilic pyrenecarboxylic acids **1–3** in CHCl_3 ^a

Compound	Absorption $\lambda_{\text{max}}/\text{nm}$ ($\epsilon/\text{M}^{-1}\text{cm}^{-1}$)	Fluorescence ^b $\lambda_{\text{max}}/\text{nm}$	Φ_f^c
1	291 (28,500), 375 (29,500), 398sh (21,400)	416, 430sh	0.81
2	287 (26,800), 363 (24,600), 389 (13,200)	407, 425sh	0.91
3	287 (28,200), 375 (26,000), 398sh (13,800)	407, 425sh	0.91

^a [Compound]= $1.2\text{--}1.5 \times 10^{-5}$ M. The absorption and fluorescence spectra of **1–3** are shown in Figure S1 (Supplementary data).

^b $\lambda_{\text{ex}}=350$ nm.

^c Fluorescence quantum yield ($\lambda_{\text{ex}}=366$ nm).

The changes in the absorption and fluorescence spectra of **1–3** with the addition of H^+ or OH^- were observed in methanol. As shown in Figure 1, in acidic methanol **1** gave the broad and less structured absorption and fluorescence spectra, while the relatively sharp and well-structured spectra were observed in basic methanol. Thus, the dependence of the absorption and fluorescence spectra of **1** on the H^+ concentration was in agreement with that of parent

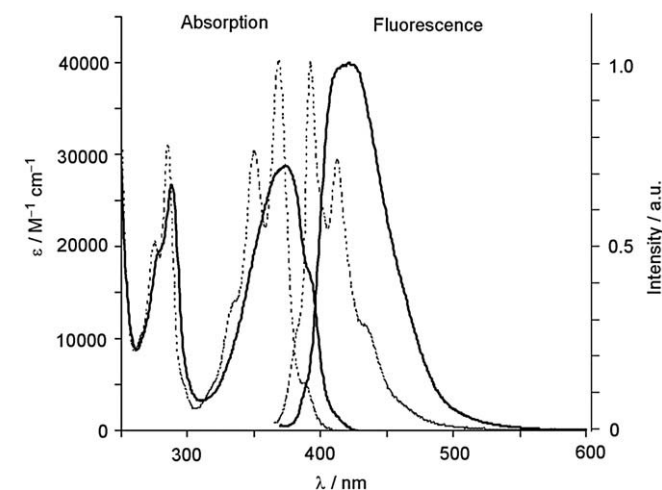


Figure 1. Absorption and fluorescence spectra of **1** in acidic (solid line) and basic (dotted line) methanol: [**1**]= 5.1×10^{-6} M, $\lambda_{\text{ex}}=350$ nm.

PyCO_2H . Similarly the spectral changes with the H^+ concentration were observed in **2** and **3**, although the positions of maximal absorption and fluorescence were shifted to shorter wavelength compared with those of **1**. The spectral data obtained in acidic and basic methanol are summarized in Table 2, together with the energy difference $\Delta\bar{\nu}$ in the maximal position of fluorescence between the basic and acidic forms. It is found that the $\Delta\bar{\nu}$ values of the amphiphilic pyrenecarboxylic acids **1–3** are slightly smaller than 2185 cm^{-1} reported for parent PyCO_2H in water,¹² suggesting that the difference in pK between the excited and ground state of **1–3** is smaller compared with that of parent PyCO_2H .

Table 2
Absorption and fluorescence spectral data of amphiphilic pyrenecarboxylic acids **1–3** in acidic and basic methanol^a

Compound	Absorption $\lambda_{\text{max}}/\text{nm}$		Fluorescence ^b $\lambda_{\text{max}}/\text{nm}$		$\Delta\bar{\nu}/\text{cm}^{-1c}$
	Acidic	Basic	Acidic	Basic	
1	288, 374, 392sh	275, 285, 350, 369	421	392, 412, 435sh	1760
2	283, 358, 385	269, 279, 335, 349	416	385, 404, 424	1940
3	283, 358, 385	269, 279, 335, 349	416	385, 404, 424	1940

^a [Compound]= $0.5\text{--}1.2 \times 10^{-5}$ M.

^b $\lambda_{\text{ex}}=350$ nm.

^c Energy difference in the maximal position of fluorescence between the basic and acidic forms.

In contrast to the good solubility in organic solvents, the amphiphilic pyrenecarboxylic acids **1–3** were hardly soluble in water. It is known that amphiphilic compounds can be dispersed in water by forming supramolecular aggregates such as micelles and bilayer membranes. However, transparent solutions could not be obtained by sonication of the amphiphiles **1–3** even in basic water.

2.3. Incorporation of amphiphilic pyrenecarboxylic acids into vesicle membrane

Next, we examined the incorporation of the amphiphilic pyrenecarboxylic acids **1–3** into vesicle membrane using 1-palmitoyl-2-oleoyl-*sn*-glycero-3-phosphocholine (POPC) as a host molecule. A vesicle solution containing the amphiphilic pyrenecarboxylic acid **1** in the vesicle membrane was prepared as follows; a suspension of **1** (0.52 μmol) and POPC (12 μmol) in 1.0 M tris(hydroxymethyl)-aminomethane-HCl (Tris-HCl) buffer (pH 7.5) was sonicated under Ar for 2 h at 10 $^\circ\text{C}$. The suspension was developed by chromatography on a Sephadex G-50 column with a buffer solution to remove **1** outside the vesicles to give a vesicle solution (11.4 mL). The formation of vesicles was confirmed by the particle size measurement with a dynamic light-scattering method, which indicated the formation of particles with a diameter of 40–200 nm in the solution. The incorporation of **1** into the vesicles was monitored by the absorption and fluorescence spectra measurements of the solution. As shown in Figure 2, a well-structured spectrum characteristic of pyrene derivatives was obtained in the absorption spectrum of the solution, indicating that the amphiphilic pyrenecarboxylic acid **1** was incorporated into the POPC vesicles in the basic form. It is noted that in the fluorescence spectrum the intensity of the peak at 392 nm was considerably reduced owing to re-absorption of the emission because the local concentration of **1** in the vesicle membrane is high. Taking into account this effect, the fluorescence spectrum of the vesicle solution is consistent with that recorded in basic methanol.

Upon acidification of the vesicle solution containing **1** by the addition of concentrated aqueous HCl, the absorption spectrum was changed to broad and the intensity of the shoulder at 393 nm assigned to the $^1A_g \rightarrow ^1L_b$ transition was increased, indicating that the carboxylate group of **1** incorporated into the vesicles was protonated instantly on addition of H^+ (Fig. 2). On the basis of the

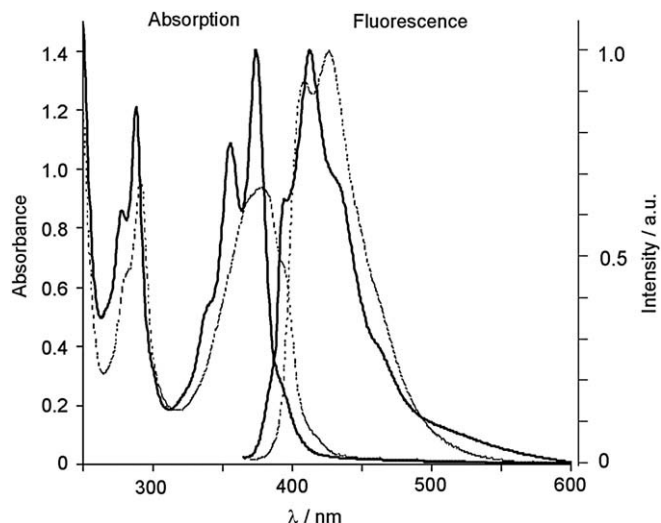


Figure 2. Absorption and fluorescence spectra of **1** incorporated into the POPC vesicle membrane in a Tris–HCl buffer solution (pH 7.5, solid line). The dotted lines display the spectra recorded after acidification (pH 0.4) by the addition of concentrated aqueous HCl. The concentration of **1** in the vesicle solution was estimated to be 40 μM . Fluorescence spectra were recorded in a quartz cell (1 mm \times 10 mm) on excitation at 350 nm.

resulting absorption spectrum of the acidic form, the concentration of **1** incorporated in the vesicle solution, C_s , could be calculated by using the molar extinction coefficient shown in Table 1, because this spectrum was practically identical to that recorded in CHCl_3 . Thus, C_s of the vesicle solution prepared under the conditions described above was determined to be 40 μM .

Similarly the pyrenecarboxylic acids **2** and **3** were incorporated into the POPC vesicle membrane. The analogous C_s values of 38–40 μM were obtained for the vesicle solutions of **2** and **3** prepared under the identical conditions to those described for **1**, suggesting that a single octyl group is hydrophobic enough to give 1-pyrenecarboxylic acid sufficient solubility in vesicle membrane. These C_s values are comparable to those of pyrenes having a moderately hydrophilic group such as 1-hydroxymethylpyrene PyCH_2OH . Moreover, the C_s value of 40 μM means that 87% of the pyrenecarboxylic acid molecules employed in the vesicle preparation are incorporated into the POPC vesicle membrane, and the fraction of the pyrenecarboxylic acid in the vesicle is estimated to be 3.8 mol% by assuming that all POPC molecules employed in the preparation are recovered in the vesicle solution.

The C_s value is, of course, dependent on the molar ratio of the pyrenecarboxylic acid to POPC in the vesicle preparation. For example, when the vesicle was prepared from **3** (4.6 μmol) and POPC (12 μmol), a solution of the vesicle containing 15 mol% of **3** was obtained ($C_s = 196 \mu\text{M}$) although the ratio of the molecules of **3** incorporated into the vesicle membrane to those employed in the vesicle preparation decreased to 49%. It is noted that in the fluorescence spectrum of the vesicle solution containing **3** in high concentration, an intense and broad peak with a maximum at 508 nm due to the excimer emission was observed (Fig. S2). Thus, we have achieved the synthesis of the pyrenecarboxylic acids having an excellent solubility in the vesicle membrane by the introduction of the hydrophobic group into the pyrene nucleus.

2.4. Ability of amphiphilic pyrenecarboxylic acids as sensitizers for electron transport across vesicle bilayers

Finally, the photoinduced electron transport across vesicle bilayers was examined by using the amphiphilic pyrenecarboxylic acids **1–3** as sensitizers. Vesicle solutions used for the electron

transport experiments were prepared in an identical manner to that described in the previous section, except that a buffer solution containing AscNa (1.0 M) was used in the vesicle preparation and $\text{MVCl}_2 \cdot 3\text{H}_2\text{O}$ was added to the outer aqueous phase. Irradiation of the vesicle solution containing the amphiphilic pyrenecarboxylic acids **1–3** with a 500-W xenon arc lamp through optical glass filters (366 \pm 15 nm) resulted in the reduction of MV^{2+} to afford $\text{MV}^{+ \cdot}$, which was readily identified by its characteristic absorption with maxima at 396 and 604 nm (Fig. 3). The sensitizer ability of **1–3** was evaluated with the initial rate of $\text{MV}^{+ \cdot}$ formation, ν_i , and the maximal concentration of photogenerated $\text{MV}^{+ \cdot}$, C_{max} , both of which were determined by the analysis of the accumulation curve of $\text{MV}^{+ \cdot}$. The result of the electron transport across vesicle bilayers obtained by using **1–3** as sensitizers is summarized in Table 3, together with that obtained by using PyCH_2OH , one of the pyrenes having high sensitizer ability,⁹ under identical irradiation conditions. The table shows that all amphiphilic pyrenecarboxylic acids **1–3** act as excellent sensitizers for the electron transport across vesicle bilayers, having larger ν_i values compared with that of PyCH_2OH .

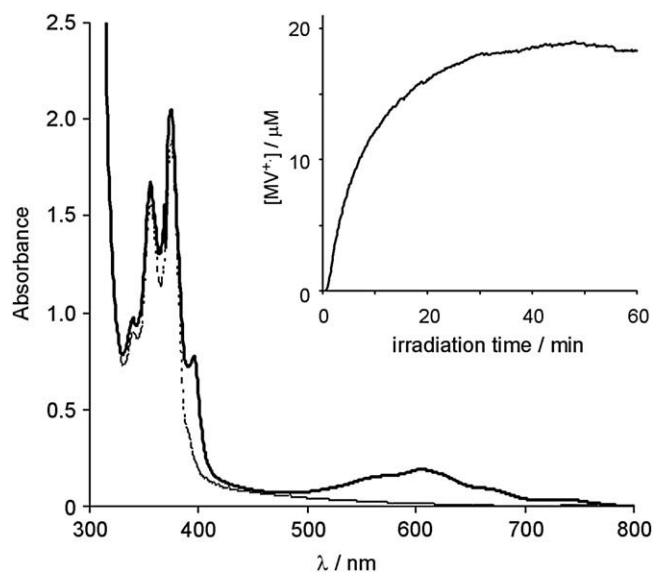


Figure 3. UV–vis absorption spectrum recorded after irradiation for 60 min of a solution of vesicles containing **1** and AscNa (solid line). The dotted line displays absorption spectrum before irradiation. The inset figure shows the change in the concentration of $\text{MV}^{+ \cdot}$ determined by the absorption at 604 nm with irradiation time.

Table 3

Electron transport across vesicle bilayers sensitized by amphiphilic pyrenecarboxylic acids **1–3**

Sensitizer	ν_i^a $10^{-6} \text{ M min}^{-1}$	C_{max}^b μM	C_s^c μM	$I(\text{rel})^d$	$\Phi_t(\text{rel})^e$
1	2.0	19.0	39	7.1	0.45
2	3.5	28.4	38	3.9	1.4
3	2.0	17.7	38	4.1	0.79
PyCH_2OH	0.62	21.6	32	1.0	1.0

^a Initial rate of $\text{MV}^{+ \cdot}$ formation.

^b Maximal concentration of photogenerated $\text{MV}^{+ \cdot}$.

^c Concentration of the sensitizer incorporated in the vesicle solution.

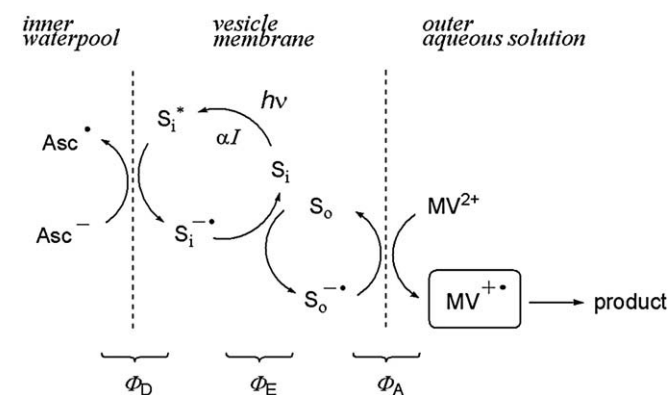
^d Estimated value of the number of photons absorbed by the sensitizer under the irradiation conditions relative to that for PyCH_2OH , see text.

^e Total quantum yield for $\text{MV}^{+ \cdot}$ formation relative to that for PyCH_2OH .

The initial rate of $\text{MV}^{+ \cdot}$ formation, ν_i , is equal to the product of the number of photons absorbed by the sensitizer in unit time, I , and a total quantum yield for $\text{MV}^{+ \cdot}$ formation, Φ_t . Thus, in order to reveal what is responsible for the increase in ν_i observed in the electron transport across vesicle bilayers by using **1–3** as sensitizers, the

relative values of I and Φ_t were evaluated and compared with those of PyCH₂OH. Since the light from a xenon arc lamp through optical glass filters (366±15 nm) was employed in the irradiation, the relative value of I for each sensitizer, $I(\text{rel})$, is estimated by the integration of $I_f(\lambda)(1 - 10^{-\varepsilon(\lambda)C_s l})$, where $I_f(\lambda)$ is the wavelength dependence of incident light evaluated by the spectrum of the light transmitted by the filters employed in the electron transport experiment, $\varepsilon(\lambda)$ is the absorption spectrum of each sensitizer recorded in basic methanol, and l is the length of the cell used in the irradiation experiment. The function $I_f(\lambda)$, as well as $\varepsilon(\lambda)$ of **1–3** and PyCH₂OH, is illustrated in Figure S3. Thus, the relative values of a total quantum yield for MV²⁺ formation, $\Phi_t(\text{rel})$, can be evaluated by $\nu_i I(\text{rel})$, which are also presented in Table 3. As shown in the table, a large increase in ν_i observed in the electron transport across vesicle bilayers by using **1–3** as sensitizers is mainly attributed to the large values of I , which is due to the bathochromic shift of their absorption maxima increasing the absorptivity of the incident light (Fig. S3).

Furthermore, it is noteworthy that a total quantum yield for MV²⁺ formation, Φ_t , in the electron transport sensitized by the amphiphilic pyrenecarboxylic acids **1–3** is larger than or comparable to that sensitized by PyCH₂OH. In analogy with the electron transport sensitized by the pyrenes having the structure of PyCH₂X (X=substituent group),⁹ we assume that the MV²⁺ formation induced by the irradiation of **1–3** proceeds by a mechanism involving the reductive quenching of the singlet excited state of the pyrene sensitizer by Asc⁻ to produce the sensitizer radical anion, followed by electron exchange between the sensitizers located at the inner and outer interfaces across the vesicle membrane (Scheme 2). The free-energy change for the reductive quenching of parent 1-pyrenecarboxylic acid PyCO₂H in the singlet excited state with Asc⁻ are calculated by the Rehm–Weller equation²⁰ to be -34 kcal mol⁻¹, and the electron transfer from the radical anion of PyCO₂H to MV²⁺ is predicted to be exothermic with the free-energy change of -28 kcal mol⁻¹.²¹ These data imply that the electron transfer processes involved in Scheme 2 are energetically favorable.



Scheme 2. Proposed mechanism for the photoinduced electron transport from Asc⁻ to MV²⁺ across vesicle membrane. S_i and S_o stand for the sensitizers located in the vesicle bilayer close to the inner waterpool and the outer aqueous phase, respectively, and Φ_D , Φ_E , and Φ_A show the efficiencies of each electron transfer process, see text.

According to this scheme, the initial rate of MV²⁺ formation, ν_i , is described by Eq. 2.

$$\nu_i = aI\Phi_D\Phi_E\Phi_A \quad (2)$$

In the equation, a is the proportion of sensitizers located at the interface of the vesicle bilayer and the inner waterpool. Furthermore, Φ_D shows the efficiency of quenching of the singlet excited state of the pyrene sensitizer S_i* by Asc⁻, which is depicted by $k_q[\text{Asc}^-]/(\tau_s^{-1} + k_q[\text{Asc}^-])$, where k_q and τ_s are the rate constant for the fluorescence quenching and the lifetime of S_i*[•], respectively. The

efficiency Φ_E represents the efficiency for the electron exchange between the sensitizers located at the inner and outer interfaces, which is equal to $k_e[\text{S}_o]/(\tau_i^{-1} + k_e[\text{S}_o])$, where k_e and τ_i are a bimolecular rate constant for an electron transfer from S_i*[•] (the radical anion of S_i) to S_o and the lifetime of S_i*[•] in the absence of S_o, respectively. Finally, Φ_A shows the efficiency for the electron transfer from S_o*[•] (the radical anion of S_o) to MV²⁺, which is depicted by $k_t[\text{MV}^{2+}]/(\tau_o^{-1} + k_t[\text{MV}^{2+}])$, where k_t and τ_o is a bimolecular rate constant for an electron transfer from S_o*[•] to MV²⁺ and the lifetime of S_o*[•] in the absence of MV²⁺, respectively. Thus, a total quantum yield for MV²⁺ formation, Φ_t , is equal to $a\Phi_D\Phi_E\Phi_A$. Unfortunately, it is difficult to specify the effect of a carboxylate group and a hydrophobic alkyl group of **1–3** on Φ_t , because these groups influence the photochemical properties of the pyrene chromophore and the position of the sensitizer in the vesicle membrane, both of which affect the efficiencies Φ_D , Φ_E , and Φ_A . However, it should be emphasized that a hydrophilic carboxylate group attached directly on the pyrene nucleus of **1–3** plays an essential role in the relatively high total efficiency Φ_t of the photoinduced electron transport across vesicle bilayers. In spite of the substitution of a long hydrophobic group, the hydrophilic carboxylate group of **1–3** anchors the pyrene chromophore at the bilayer–water interface rigidly, the position of which is favorable for the interaction with Asc⁻ and MV²⁺ in aqueous phases to increase Φ_D and Φ_A by an increase in k_q and k_t , respectively.

3. Conclusion

In order to employ pyrenecarboxylic acids as sensitizers for the electron transport across vesicle bilayers, we designed the novel pyrenecarboxylic acids **1–3** having a single or double hydrophobic alkyl chain, which were expected to have good solubility in vesicle membrane, and achieved their syntheses by using 1,6-dibromopyrene as a starting material. The amphiphilic pyrenecarboxylic acids **1–3** were fairly soluble in organic solvents such as CHCl₃ and methanol. In analogy with parent 1-pyrenecarboxylic acid PyCO₂H, the significant changes in the absorption and fluorescence spectra of **1–3** with the addition of H⁺ or OH⁻ were observed in methanol. As expected, the introduction of a hydrophobic alkyl group into the pyrene nucleus of PyCO₂H caused a significant increase in solubility in the vesicle membrane, so that the sonication of **1–3** with POPC in a buffer solution followed by gel filtration afforded a vesicle solution containing **1–3** in the vesicle membrane. The fraction of the amphiphilic pyrenecarboxylic acid molecules incorporated into the vesicle to those employed in the vesicle preparation was comparable to that of the pyrene having a moderately hydrophilic group such as 1-hydroxymethylpyrene PyCH₂OH. Finally, we found that the amphiphilic pyrenecarboxylic acids **1–3** acted as excellent sensitizers for the electron transport across vesicle bilayers. The carboxylate group contributes essentially to the enhancement of the initial rate of MV²⁺ formation because it causes the bathochromic shift of the absorption maxima of the sensitizers and it anchors the pyrene chromophore at the bilayer–water interface. Moreover, it would be expected that the novel pyrenes described in this paper, which have good solubility in hydrophobic membrane and exhibit a spectroscopic response to the H⁺ concentration, are useful as probes to characterize the properties of various multi-molecular systems.

4. Experimental

4.1. General

¹H and ¹³C NMR spectra were recorded on a JEOL JNM-A500, ECA-500, ECX-400, or EX-270 spectrometer. Chemical shifts are reported in parts per million from tetramethylsilane. High resolution mass

spectra (HRMS) were recorded on a JEOL JMS-700 mass spectrometer under fast atom bombardment (FAB) conditions using NBA as a matrix. UV–visible absorption spectra were recorded on a JASCOV-560 spectrometer with a 400 nm min⁻¹ scanning speed and a 2.0 nm bandwidth. Fluorescence spectra were recorded on a JASCO FP-777 spectrofluorometer with a 200 nm min⁻¹ scanning speed and a 1.5 nm bandwidth. The distribution of the particle size in vesicle solutions was measured by using Honeywell Microtrac UPA-150 at room temperature. Gel permeation liquid chromatography (GPC) was performed on a Nippon Bunseki Kogyo LC-08 equipped with two JAIGEL-H columns. For column chromatography Kanto Chemical Co., Inc. silica gel 60 N (40–100 mesh) was used. Preparative thin-layer chromatography (PTLC) was performed on Merck silica gel 60 F₂₅₄. 1-Palmitoyl-2-oleoyl-*sn*-glycero-3-phosphocholine (POPC) was purchased from Avanti Polar Lipids and used without purification. *N,N'*-Dimethyl-4,4'-bipyridinium dichloride trihydrate (MVCl₂·3H₂O), sodium ascorbate (AscNa), and tris(hydroxymethyl)aminomethane (Tris) were purchased from Tokyo Kasei Kogyo Co., Ltd. and used without purification. Quinine sulfate employed as a standard for quantum yield determination was recrystallized from water.

4.2. Preparation of the amphiphilic pyrenecarboxylic acids 1–3

4.2.1. 6-(1-Octynyl)-1-pyrenecarboxylic acid (1)

A suspension of 1,6-dibromopyrene¹⁵ (177.7 mg, 0.494 mmol), PdCl₂(PPh₃)₂ (17.8 mg, 0.0254 mmol), and CuI (2.4 mg, 0.013 mmol) in morpholine (5 mL) was stirred at 0 °C for 10 min. 1-Octyne (80 μL, 0.544 mmol) was added to the suspension, and the resultant mixture was stirred at 100 °C for 22.5 h. The mixture was cooled to room temperature and filtered. The filtrate was concentrated under reduced pressure. Purification by column chromatography on silica gel (hexane) afforded 1-bromo-6-(1-octynyl)pyrene (54.0 mg, 0.139 mmol, 28%): ¹H NMR (270 MHz, CDCl₃) δ 8.52 (d, *J*=9.2 Hz, 1H), 8.34 (d, *J*=9.2 Hz, 1H), 8.18 (d, *J*=8.4 Hz, 1H), 8.06–7.93 (m, 5H), 2.65 (t, *J*=7.0 Hz, 2H), 1.80–1.72 (m, 2H), 1.62–1.57 (m, 2H), 1.43–1.37 (m, 4H), 0.95 (t, *J*=7.0 Hz, 3H). To a solution of 1-bromo-6-(1-octynyl)pyrene (54.0 mg, 0.139 mmol) in THF (4 mL) was added *n*-BuLi (1.58 M in hexane solution, 0.2 mL, 0.316 mmol) at –78 °C, and the resultant mixture was stirred at the same temperature for 10 min. To the solution was added crumbled dry ice (ca.10 g, 227 mmol) at once, and the mixture was stirred at –78 °C for 30 min. After being stirred at room temperature for 40 min, the reaction mixture was quenched with 1 M HCl and extracted with ether. The organic layer was separated, washed with brine, dried over Na₂SO₄, filtered, and concentrated under reduced pressure. Purification by PTLC (hexane–diethyl ether 2:3) afforded **1** (31.6 mg, 0.0891 mmol, 64%) as a yellow solid: mp 215 °C; ¹H NMR (270 MHz, CDCl₃) δ 9.40 (d, *J*=9.2 Hz, 1H), 8.80 (d, *J*=8.4 Hz, 1H), 8.73 (d, *J*=8.9 Hz, 1H), 8.25–8.13 (m, 5H), 2.67 (t, *J*=7.0 Hz, 2H), 1.85–1.74 (m, 2H), 1.58 (br, 2H), 1.45–1.39 (m, 4H), 0.96 (t, *J*=6.8 Hz, 3H); ¹³C NMR (125 MHz, CDCl₃) δ 171.7, 135.1, 132.0, 131.7, 130.1, 129.72, 129.67, 129.6, 129.4, 128.4, 127.7, 125.9, 125.2, 124.7, 124.5, 121.9, 120.8, 97.5, 79.4, 31.4, 28.9, 28.8, 22.6, 20.0, 14.1; HRMS (FAB) calcd for C₂₅H₂₁O₂Na [(M–H+2Na)⁺] 399.1337, found 399.1362.

4.2.2. 6-Octyl-1-pyrenecarboxylic acid (2)

A mixture of 1-bromo-6-(1-octynyl)pyrene (98.8 mg) and PtO₂ (15.4 mg) in ethyl acetate (10 mL) was stirred at room temperature under H₂ atmosphere for 1 h. The catalyst was filtered through a plug of Celite with ethyl acetate, and the filtrate was concentrated under reduced pressure to give 1-bromo-6-octylpyrene (90.5 mg, 92%): ¹H NMR (500 MHz, CDCl₃) δ 8.39 (d, *J*=9.2 Hz, 1H), 8.31 (d, *J*=9.2 Hz, 1H), 8.22 (d, *J*=8.0 Hz, 1H), 8.16 (d, *J*=8.5 Hz, 1H), 8.15 (d, *J*=9.4 Hz, 1H), 8.06 (d, *J*=9.0 Hz, 1H), 8.00 (d, *J*=8.5 Hz, 1H), 7.91 (d,

J=7.8 Hz, 1H), 3.34 (dd, *J*=7.8 Hz, 2H), 1.85 (m, 2H), 1.49 (m, 2H), 1.38 (m, 2H), 1.28 (m, 6H), 0.88 (t, *J*=6.7 Hz, 3H). To a solution of 1-bromo-6-octylpyrene (90.5 mg) in THF (10 mL) was added *n*-BuLi (1.57 M in hexane solution, 0.4 mL, 0.628 mmol) at –78 °C, and the resulting mixture was stirred at the same temperature for 10 min. To the solution was added crumbled dry ice (ca. 3 g, 68 mmol) at once, and the mixture was stirred at –78 °C for 30 min. After being stirred at room temperature for 30 min, the reaction mixture was quenched with 1 M HCl and extracted with ether. The organic layer was separated, washed with brine, dried over Na₂SO₄, filtered, and concentrated under reduced pressure. Purification by PTLC (CHCl₃–methanol 50:1) gave yellow solid (crude, 67.8 mg). The crude solid was purified by GPC (CHCl₃) afforded **2** (26.5 mg, 0.0739 mmol, 16%) as a pale yellow solid: mp 183 °C; ¹H NMR (270 MHz, CDCl₃) δ 9.34 (d, *J*=9.4 Hz, 1H), 8.76 (d, *J*=8.0 Hz, 1H), 8.45 (d, *J*=9.2 Hz, 1H), 8.24 (d, *J*=9.4 Hz, 1H), 8.23 (d, *J*=8.1 Hz, 1H), 8.19 (d, *J*=8.2 Hz, 1H), 8.14 (d, *J*=9.2 Hz, 1H), 7.95 (d, *J*=7.8 Hz, 1H), 3.38 (t, *J*=8.1 Hz, 2H), 1.87 (quin, *J*=8.0 Hz, 2H), 1.50 (m, 2H), 1.33–1.25 (m, 6H), 0.88 (t, *J*=6.9 Hz, 3H); ¹³C NMR (125 MHz, CDCl₃) δ 170.8, 139.3, 134.9, 134.6, 132.3, 130.0, 129.2, 128.8, 128.5, 127.9, 126.8, 126.4, 126.2, 123.9, 123.8, 33.8, 32.3, 31.9, 29.7, 29.5, 29.3, 14.1; HRMS (FAB) calcd for C₂₅H₂₅O₂Na [(M–H+2Na)⁺] 403.1650, found 403.1656.

4.2.3. 6-(3,4-Didodecyloxy-1-butyl)-1-pyrenecarboxylic acid (3)

A suspension of 1,6-dibromopyrene¹⁵ (2.20 g, 6.11 mmol), PdCl₂(PPh₃)₂ (57.2 mg, 0.0815 mmol), and CuI (8.6 mg, 0.045 mmol) in morpholine (60 mL) was stirred at 0 °C for 10 min. To the suspension was added a solution of 4-ethynyl-2,2-dimethyl-1,3-dioxolane²⁴ (514.7 mg, 4.08 mmol) in morpholine (2 mL), and the resultant mixture was stirred at 100 °C for 18 h. The mixture was cooled to room temperature and filtered. The filtrate was concentrated under reduced pressure. Purification by column chromatography on silica gel (hexane–ethyl acetate 4:1) afforded 1-bromo-6-[2-(2,2-dimethyl-1,3-dioxolan-4-yl)-1-ethynyl]pyrene (0.53 g, 1.31 mmol, 32%) as a yellow solid: mp 40 °C; ¹H NMR (500 MHz, CDCl₃) δ 8.51 (d, *J*=9.2 Hz, 1H), 8.43 (d, *J*=8.1 Hz, 1H), 8.23 (d, *J*=8.1 Hz, 1H), 8.15–8.07 (m, 4H), 8.02 (d, *J*=8.0, 1H), 5.19 (t, *J*=6.4 Hz, 1H), 4.39 (dd, *J*=7.2, 6.5 Hz, 1H), 4.23 (dd, *J*=7.8, 6.9 Hz, 1H), 1.65 (s, 3H), 1.50 (s, 3H); ¹³C NMR (125 MHz, CDCl₃) δ 131.2, 130.7, 130.43, 130.39, 129.7, 128.7, 128.1, 126.8, 126.2, 126.1, 125.9, 125.6, 125.4, 124.9, 123.7, 120.6, 117.5, 110.6, 92.5, 84.6, 70.3, 66.4, 26.4, 26.1. To a solution of 1-bromo-6-[2-(2,2-dimethyl-1,3-dioxolan-4-yl)-1-ethynyl]pyrene (0.32 g, 0.79 mmol) in THF (6 mL) was added 4 M HCl (1.2 mL), and the resultant solution was stirred at room temperature for 22 h. The reaction mixture was quenched with saturated aqueous NaHCO₃ and concentrated under reduced pressure. Purification by column chromatography on silica gel (CHCl₃–methanol 4:1) gave 1-bromo-6-(3,4-dihydroxy-1-butyn-1-yl)pyrene (321.7 mg, quant.) as a pale yellow solid: mp 187 °C; ¹H NMR (500 MHz, CDCl₃) δ 8.54 (d, *J*=9.2 Hz, 1H), 8.49 (d, *J*=9.2 Hz, 1H), 8.28 (d, *J*=8.0 Hz, 1H), 8.17–8.12 (m, 4H), 8.08 (d, *J*=8.2 Hz, 1H), 4.95–4.92 (m, 1H), 4.05–3.95 (m, 2H), 2.53 (d, *J*=6.0 Hz, 1H), 2.21 (dd, *J*=7.8, 5.3 Hz, 1H); ¹³C NMR (125 MHz, CDCl₃-CD₃OD (*v/v*=3:2)) δ 131.7, 130.8, 130.2, 130.1, 130.0, 129.4, 128.4, 127.7, 126.4, 125.8, 125.7, 125.3, 125.1, 124.6, 123.4, 120.1, 93.3, 83.5, 66.1, 63.5; HRMS (FAB) calcd for C₂₀H₁₃BrO₂Na [(M+Na)⁺] 386.9997, found 386.9997. To a solution of 1-bromo-6-(3,4-dihydroxy-1-butyn-1-yl)pyrene (162.0 mg, 0.444 mmol) in DMF (5 mL) was added NaH (including mineral oil, 39.3 mg, 0.983 mmol) at 0 °C, and the resultant mixture was stirred at the same temperature for 30 min. To the solution was added 1-bromododecane (0.43 mL, 1.79 mmol). The resultant mixture was stirred at 0 °C for 30 min, then at room temperature for 2.5 h. The reaction mixture was quenched with saturated aqueous NH₄Cl, extracted with ether. The organic layer was washed with brine, dried over Na₂SO₄, filtered, and concentrated under reduced pressure. Purification by column chromatography on silica gel (hexane–ethyl

acetate 25:1) afforded 1-bromo-6-(3,4-didodecyloxy-1-butyn-1-yl)pyrene (127.8 mg, 0.182 mmol, 41%) as yellow viscous oil: $^1\text{H NMR}$ (500 MHz, CDCl_3) δ 8.59 (d, $J=9.2$ Hz, 1H), 8.47 (d, $J=9.4$ Hz, 1H), 8.26 (d, $J=8.0$ Hz, 1H), 8.15 (s, 2H), 8.15 (d, $J=9.2$ Hz, 1H), 8.11 (d, $J=9.4$ Hz, 1H), 8.06 (d, $J=8.2$ Hz, 1H), 4.68 (dd, $J=6.4, 5.0$ Hz, 1H), 3.97 (ddd, $J=9.4, 6.6, 6.6$ Hz, 1H), 3.864 (d, $J=6.4$ Hz, 1H), 3.860 (d, $J=5.0$ Hz, 1H), 3.69–3.62 (m, 3H), 1.75–1.63 (m, 4H), 1.43–1.21 (m, 36H), 0.87 (t, $J=6.9$ Hz, 3H), 0.86 (t, $J=6.9$ Hz, 3H); $^{13}\text{C NMR}$ (125 MHz, CDCl_3) δ 133.2, 131.8, 131.1, 130.51, 130.47, 130.4, 128.8, 128.0, 126.8, 126.1, 125.8, 125.5, 120.6, 118.1, 84.9, 77.3, 72.0, 70.2, 69.8, 31.9, 29.73, 29.71, 29.66, 29.6, 29.55, 29.51, 29.3, 26.20, 26.16, 22.7, 14.1; HRMS (FAB) calcd for $\text{C}_{44}\text{H}_{61}\text{BrO}_2\text{Na}$ [(M+Na) $^+$] 723.3753, found 723.3730. A mixture of 1-bromo-6-(3,4-didodecyloxy-1-butyn-1-yl)pyrene (88.0 mg, 0.125 mmol) and PtO_2 (10.3 mg) in ethyl acetate (3 mL) was stirred at room temperature under H_2 atmosphere for 80 min. The catalyst was filtered through a plug of Celite with ethyl acetate, and the filtrate was concentrated under reduced pressure to give 1-bromo-6-(3,4-didodecyloxy-1-butyl)pyrene (88.0 mg, quant.) as pale yellow viscous oil: $^1\text{H NMR}$ (500 MHz, CDCl_3) δ 8.39 (d, $J=9.2$ Hz, 1H), 8.37 (d, $J=9.2$ Hz, 1H), 8.16 (d, $J=8.9$ Hz, 1H), 8.14 (d, $J=9.4$ Hz, 1H), 8.05 (d, $J=9.4$ Hz, 1H), 8.00 (d, $J=8.3$ Hz, 1H), 7.93 (d, $J=7.8$ Hz, 1H), 3.69 (ddd, $J=9.2, 6.7, 6.2$ Hz, 1H), 3.57–3.35 (m, 10H), 2.06 (br, 2H), 1.69–1.63 (m, 2H), 1.58–1.52 (m, 2H), 1.46–1.39 (m, 2H), 1.23 (br, 32H), 0.870 (t, $J=6.9$ Hz, 3H), 0.865 (t, $J=7.1$ Hz, 3H); $^{13}\text{C NMR}$ (125 MHz, CDCl_3) δ 130.4, 130.0, 129.9, 129.1, 128.8, 127.9, 126.9, 126.5, 126.3, 125.4, 125.2, 125.1, 124.5, 124.2, 123.9, 116.0, 78.0, 77.4, 73.0, 71.7, 70.3, 34.4, 31.9, 30.3, 29.70, 29.69, 29.67, 29.63, 29.61, 29.58, 29.5, 29.4, 29.3, 26.3, 26.2, 22.7, 14.1. To a solution of 1-bromo-6-(3,4-didodecyloxy-1-butyl)pyrene (100.9 mg, 0.143 mmol) in THF (4 mL) was added *n*-BuLi (1.57 M in hexane solution, 0.15 mL, 0.236 mmol) at -78°C , then the resultant solution was stirred at same temperature for 10 min. To the solution was added crumbled dry ice (ca. 10 g, 227 mmol) at once, and the mixture was stirred at -78°C for 30 min. After being stirred at room temperature for 1.5 h, the reaction mixture was quenched with 1 M HCl and extracted with ether. The organic layer was separated, washed with brine, dried over Na_2SO_4 , filtered, and concentrated under reduced pressure. Purification by PTLC (CHCl_3 –methanol 30:1) gave a yellow solid (68.8 mg). The crude solid was purified by GPLC (CHCl_3) to afford **3** (52.2 mg, 0.0778 mmol, 54%) as a pale yellow solid: mp 67°C ; $^1\text{H NMR}$ (500 MHz, CDCl_3) δ 9.35 (d, $J=9.5$ Hz, 1H), 8.76 (d, $J=8.3$ Hz, 1H), 8.51 (d, $J=9.2$ Hz, 1H), 8.24 (d, $J=9.8$ Hz, 1H), 8.23 (d, $J=8.0$ Hz, 1H), 8.18 (d, $J=8.3$ Hz, 1H), 8.13 (d, $J=9.2$ Hz, 1H), 7.97 (d, $J=7.6$ Hz, 1H), 3.70 (ddd, $J=8.9, 6.7, 6.4$ Hz, 1H), 3.62–3.38 (m, 10H), 2.08 (br, 2H), 1.70–1.54 (m, 4H), 1.46–1.40 (m, 2H), 1.23 (br, 32H), 0.870 (t, $J=6.7$ Hz, 3H), 0.865 (t, $J=6.7$ Hz, 3H); $^{13}\text{C NMR}$ (100 MHz, CDCl_3) δ 172.9, 138.8, 134.9, 132.2, 130.0, 129.4, 128.9, 128.6, 127.9, 127.0, 126.4, 126.2, 125.2, 124.6, 124.0, 123.9, 121.6, 78.0, 77.3, 73.0, 71.7, 70.4, 34.6, 31.9, 30.3, 29.7, 29.62, 29.59, 29.5, 29.4, 26.3, 26.2, 22.7, 14.1; HRMS (FAB) calcd for $\text{C}_{45}\text{H}_{65}\text{O}_4\text{Na}_2$ [(M–H+2Na) $^+$] 715.4678, found 715.4688.

4.3. Absorption and fluorescence spectra measurements

Absorption and fluorescence spectra were measured for a solution of the amphiphilic pyrenecarboxylic acids **1–3** at 10^{-5} M concentration in CHCl_3 (3 mL) in a quartz cell (10 mm \times 10 mm). Fluorescence spectra were recorded on excitation at 350 nm. The spectra of **1–3** in the acidic and basic form were measured for a solution at 10^{-5} M concentration in methanol (3 mL) containing HCl (10^{-3} M) prepared by dilution of 12 M HCl with methanol and a solution in methanol containing NaOH (10^{-2} M). Measurements of fluorescence quantum yields were carried out for CHCl_3 solutions of **1–3** at 10^{-6} M concentration in a quartz cell (10 mm \times 10 mm) under air. All the spectra were recorded on excitation at 366 nm, and emission and excitation bandwidths were set at 1.5 nm. Quantum yields were determined by using Eq. 3,

$$\Phi_x = \Phi_{\text{st}} \frac{\text{FA}_x \text{Abs}_{\text{st}} I_{\text{st}} \left(\frac{n_x}{n_{\text{st}}}\right)^2}{\text{FA}_{\text{st}} \text{Abs}_x I_x} \quad (3)$$

where Φ is a fluorescence quantum yield, FA is an emission peak area, Abs is an optical density at the excitation wavelength, n is a refractive index of solvent, I is the light intensity at the excitation wavelength, and both x and st are subscripts denoting an unknown sample (amphiphilic pyrenecarboxylic acids) and a standard, respectively. A solution of quinine sulfate in 1 N H_2SO_4 was used as a standard ($\Phi_{\text{st}}=0.55$).

4.4. Vesicle preparation

A chloroform solution of POPC (12 μmol) and the amphiphilic pyrenecarboxylic acids **1–3** (0.52 μmol) was concentrated under reduced pressure to form a thin film in a flask. The film was dried under vacuum overnight, and then dispersed in a 1.0 M Tris–HCl buffer (pH 7.5, 4 mL) by vortex mixing (Sibata, TTM-1). After Ar was bubbled for 10 min, the resulting suspension was treated with ultrasonic process (Iwaki, USC-100Z38S-22) under Ar for 2 h at 10°C . The solution was developed on a column with Sephadex G-50 (Amersham Biosciences) equilibrated with a 1.0 M Tris–HCl buffer solution, and the fraction containing **1–3** was collected to give the vesicle solution (11.4 mL). A vesicle solution for electron transport experiments was prepared in the same manner as that described above, except for the use of a 1.0 M Tris–HCl buffer solution containing 1.0 M AscNa in the vesicle preparation and a 1.0 M Tris–HCl buffer solution containing 1.0 M NaCl as the eluent of column chromatography. After removal of AscNa and the sensitizer outside the vesicles by the chromatography, $\text{MVCl}_2 \cdot 3\text{H}_2\text{O}$ was added to give a vesicle solution for electron transport experiments with MV^{2+} (10 mM) in an outer aqueous phase. The concentration of the sensitizer in the vesicle solution, C_s , was evaluated by the absorbance at the wavelength of its maximal absorption after the addition of 12 M HCl (10% v/v of the vesicle solution) and its molar extinction coefficient determined in CHCl_3 .

4.5. Photochemistry

A vesicle solution (3 mL) was placed in a quartz cell (10 mm \times 10 mm), and Ar was bubbled into the solution for 1 h. The solution was irradiated using a 500-W xenon arc lamp through both a band-pass (360 \pm 20 nm) and a cut-off filter (>350 nm). The light intensity at the cell position was measured by the use of a photon counting meter (Ushio, UIT-150) and adjusted to 1.00 mW cm^{-2} at 365 nm. The accumulation of MV^{+} was monitored by an increase in the absorption at 604 nm, and the concentration of MV^{+} , $[\text{MV}^{+}]$, was calculated by using its molar extinction coefficient ($\epsilon=12,400 \text{ M}^{-1} \text{ cm}^{-1}$).²⁵ An increase in $[\text{MV}^{+}]$ with irradiation time, t , obeyed good first-order kinetics (Eq. 4), from which the initial rate of MV^{+} formation, ν_i , was calculated as $A_m k_{\text{obs}}$.

$$[\text{MV}^{+}] = A_m [1 - \exp(-k_{\text{obs}} t)] \quad (4)$$

Acknowledgements

This work was supported by a Grant-in-Aid for Scientific Research 20550119 from the Japan Society for the Promotion of Science. This work was also supported by Research Fellowships of 21st century COE program for Frontiers of fundamental chemistry from the Ministry of Education, Culture, Sports, Science, and Technology of Japan.

Supplementary data

Electronic Supplementary data (ESI) on absorption and fluorescence spectra of **1–3** in CHCl_3 , absorption and fluorescence

spectra of **3** incorporated into the POPC vesicle membrane in a Tris–HCl buffer solution, and absorption spectra of **1–3** in basic methanol as well as that of PyCH₂OH in CHCl₃ is available free of charge. Supplementary data associated with this article can be found in the online version, at doi:10.1016/j.tet.2009.07.033.

References and notes

1. Murov, S. L.; Carmichael, I.; Hug, G. L. *Handbook of Photochemistry*, 2nd ed.; Marcel Dekker: New York, NY, 1993.
2. Dong, D. C.; Winnik, M. A. *Photochem. Photobiol.* **1982**, *35*, 17; Dong, D. C.; Winnik, M. A. *Can. J. Chem.* **1984**, *62*, 2560.
3. For a review of photophysics of pyrenes in organized media, see: Winnik, F. M. *Chem. Rev.* **1993**, *93*, 587.
4. Duhamel, J.; Kanagalingam, S.; O'Brien, T. J.; Ingrassia, M. W. *J. Am. Chem. Soc.* **2003**, *125*, 12810.
5. Karpovich, D. S.; Blanchard, G. J. *Langmuir* **1996**, *12*, 5522.
6. Galla, H.-J.; Hartmann, W.; Theilen, U.; Sackmann, E. *J. Membr. Biol.* **1979**, *48*, 215; Somerharju, P. J.; Virtanen, J. A.; Eklund, K. K.; Vainio, P.; Kinnunen, P. K. *J. Biochemistry* **1985**, *24*, 2773; Hresko, R. C.; Sugár, I. P.; Barenholz, Y.; Thompson, T. E. *Biochemistry* **1986**, *25*, 3813; Barenholz, Y.; Cohen, T.; Haas, E.; Ottolenghi, M. *J. Biol. Chem.* **1996**, *271*, 3085.
7. Murata, S.; Nakatsuji, R.; Tomioka, H. *J. Chem. Soc., Perkin Trans. 2* **1995**, 793; Ikeda, S.; Murata, S.; Ishii, K.; Hamaguchi, H. *Bull. Chem. Soc. Jpn.* **2000**, *73*, 2483.
8. Yoshida, A.; Harada, A.; Mizushima, T.; Murata, S. *Chem. Lett.* **2003**, *32*, 68.
9. Mizushima, T.; Yoshida, A.; Harada, A.; Yoneda, Y.; Minatani, T.; Murata, S. *Org. Biomol. Chem.* **2006**, *4*, 4336.
10. Milisavljevic, B. H.; Thomas, J. K. *J. Phys. Chem.* **1988**, *92*, 2997.
11. Yao, C.; Kraatz, H.-B.; Steer, R. P. *Photochem. Photobiol. Sci.* **2005**, *4*, 191.
12. Zelent, B.; Vanderkooi, J. M.; Coleman, R. G.; Gryczynski, I.; Gryczynski, Z. *Biophys. J.* **2006**, *91*, 3864.
13. Nucci, N. V.; Zelent, B.; Vanderkooi, J. M. *J. Fluoresc.* **2008**, *18*, 41.
14. Kano, K.; Ishimura, T.; Hashimoto, S. *J. Phys. Chem.* **1991**, *95*, 7839.
15. Grimshaw, J.; Grinshaw, J. T. *J. Chem. Soc., Perkin Trans. 1* **1972**, 1622.
16. For a review of synthetic bilayer membranes: see Kunitake, T. *Angew. Chem., Int. Ed. Engl.* **1992**, *31*, 709.
17. Vander Donckt, E.; Dramaix, R.; Nasielski, J.; Vogels, C. *Trans. Faraday Soc.* **1969**, *65*, 3258.
18. Escabi-Perez, J. R.; Fendler, J. H. *J. Am. Chem. Soc.* **1978**, *100*, 2234.
19. Förster, T. *Z. Elektrochim. Angew. Physik. Chem.* **1950**, *54*, 531.
20. Rehm, D.; Weller, A. *Isr. J. Chem.* **1970**, *8*, 259.
21. For the calculation of the free-energy change for the electron transfer process, -1.67 V, $+0.09$ V, and -0.46 V were employed for the reduction potential of PyCO₂H²² and the redox potentials of Asc[•]/Asc^{•-} (pH 7.0)²³ and MV²⁺/MV^{•+} (vs SCE), respectively. The 0,0 transition energy of PyCO₂H was evaluated by the absorption spectrum of its basic form (381 nm, see text) to be 75.0 kcal mol⁻¹.
22. Fukuzumi, S.; Hironaka, K.; Nishizawa, N.; Tanaka, T. *Bull. Chem. Soc. Jpn.* **1983**, *56*, 2220.
23. Njus, D.; Kelly, P. M. *Biochim. Biophys. Acta* **1993**, *1144*, 235.
24. Deng, Y.; Salomon, R. G. *J. Org. Chem.* **2000**, *65*, 6660.
25. Ford, W. E.; Otvos, J. W.; Calvin, M. *Nature* **1978**, *274*, 507; Steckhan, E.; Kuwana, T. *Ber. Bunsenges.* **1974**, *78*, 253.